

1 **Isotopic differences of soil-plant-atmosphere continuum**  
2 **composition and control factors of different vegetation zones**  
3 **in north slope of Qilian Mountains**

4 Yuwei Liu<sup>a,b</sup>, Guofeng Zhu<sup>a,b,\*</sup>, Zhuangxia Zhang<sup>a,b</sup>, Zhigang Sun<sup>a,b</sup>, Leilei Yong<sup>a,b</sup>,  
5 Liyuan Sang<sup>a,b</sup>, Lei Wang<sup>a,b</sup>, Kailiang Zhao<sup>a,b</sup>

6 a School of Geography and Environment Science, Northwest Normal University, Lanzhou 730070,  
7 Gansu, China

8 b Shiyang River Ecological Environment Observation Station, Northwest Normal University, Lanzhou  
9 730070, Gansu, China

10 *Correspondence to:* Guofeng Zhu (gfzhu@lzb. ac.cn)

11 **Abstract:** Understanding the differences and controlling factors of stable water isotopes in the  
12 soil-plant-atmosphere continuum (SPAC) of different vegetation zones is of great guiding significance  
13 for revealing hydrological processes and regional water cycle mechanisms. From April 2018 to October  
14 2019, we collected 1281 samples in the Shiyang River Basin. In this study, we **investigated** the changes  
15 of stable water isotopes in the **SPAC** in three different vegetation zones (alpine meadow, forest, and  
16 arid foothills) in the Shiyang River Basin. The results show that: (1) In SPAC, precipitation isotope has  
17 the main controlling effect. From alpine meadows to arid foothills, **the temperature effect of**  
18 **precipitation isotopes increases with the decrease of altitude.** (2) **The soil water isotope is gradually**  
19 **enriched from the alpine meadow to the arid foothills.** (3) Alpine meadow plants are mainly supplied  
20 by precipitation in the rainy season, and forest plants mainly utilize soil water in the dry season and  
21 precipitation in the rainy season. **The soil water in the arid foothills is primarily recharged by**  
22 **groundwater, and the evaporation of plant isotopes is strong.** (4) Temperature and altitude are potential  
23 factors that control the isotope composition of SPAC. This research will help understand the SPAC  
24 system's water cycle at different altitudes and climates in high mountains.

25 **Keywords:** Shiyang River Basin; Stable isotope; Precipitation; Soil water; Plant water

26 **1 Introduction**

27 **The relative abundance changes of oxygen and hydrogen isotopes in water can indicate the water**

28 cycle and the water use mechanism in plants, so isotope technology has become an increasingly  
29 important method for studying the water cycle (Gao et al., 2009; Song et al., 2002; Coplen, 2013; Shou  
30 et al., 2013). The stable isotope composition of water is considered to be the “fingerprint” of water,  
31 which records a large amount of environmental information that comprehensively reflects the  
32 geochemical process of each system, and links the composition characteristics of each link (Darling et  
33 al., 2003; Raco et al., 2013; Nlend et al., 2020). As an effective tool, stable isotope technology is  
34 widely applied in studying the relationship between environmental factors and the water cycle  
35 (Araguás-Araguás et al., 1998; Christopher et al., 2009), water transportation, and distribution  
36 mechanisms (Gao et al., 2011), and ways of tracing water use by plants (Detjen et al., 2015). The  
37 understanding of the relationship between the influence of plant characteristics, water use efficiency  
38 and water sources (Ehleringer, 1991; Sun et al., 2005; Li et al., 2019) provides a new observation  
39 method for revealing the water cycle mechanism of the hydrological ecosystem (Nie et al., 2014; Yu et  
40 al., 2007; Wang et al., 2019)

41 Although the isotope ratio in soil water varies with depth, it remains stable when transferred from  
42 plant roots to stems, leaves or young unbolted branches (Porporato, 2001; Meissner et al., 2014).  
43 Combined the isotopic composition changes of surface water, soil water and groundwater, precipitation  
44 infiltration and runoff generation process (Bam and Ireso, 2018; Hou et al., 2008), groundwater  
45 recharge and regeneration capacity (Smith et al., 1992; Cortes and Farvolden, 1989) can be determined.  
46 Regional meteorological and hydrological conditions and the contribution of various environmental  
47 factors can be evaluated (Hua et al., 2019) by comparing different waterline equations and analyzing  
48 changes in various water bodies. Furthermore, it has laid a foundation for studying the deep mechanism  
49 of the water cycle (Gao et al., 2009). As an important component of the global water cycle, plants  
50 control 50-90% of transpiration (Jasechko et al., 2013; Coenders-Gerrits et al., 2014; Schlesinger and  
51 Jasechko, 2014). The roots of plants have no isotope fractionation when absorbing water (White et al.,  
52 1985; Song et al., 2013), so the water isotope composition of plant roots and stems reflects the isotope  
53 composition of water available for plants (Dawson et al., 1991).

54 The research of the water cycle based on SPAC plays a vital role in the study of water in arid areas  
55 and the sources of plant water use (Price et al., 2012; Shou et al., 2013). Hydrogen and oxygen isotopes  
56 have been used to study the water cycle at the interface of "soil-root", "soil-plant", and  
57 "soil-atmosphere", but only a few parameters play an important role in the complex interactions

58 between various surfaces (Durand et al., 2007; Li et al., 2006; West et al., 2010). Previous studies have  
59 shown that local factors, especially temperature, mainly control stable isotope precipitation changes in  
60 mid-latitudes (Dai et al., 2020). Through the research on the composition of hydrogen and oxygen  
61 isotopes in different water bodies, we can further understand the mechanism of water use by vegetation  
62 (Yang et al., 2015) and provide a scientific basis for vegetation restoration in arid and semi-arid areas.  
63 In the existing research, how to extend the results of the small-scale SPAC water cycle research to the  
64 large-scale area has become a hot spot and difficulty. In inland arid areas, due to the lack of water  
65 resources, the exchange of energy and water with the outside world is small, and the water cycle is  
66 mainly the vertical circulation of groundwater-soil-atmospheric water. Therefore, studying the changes  
67 in SPAC isotopic composition in arid regions is significant for ecological restoration.

68 The Shiyang River Basin has the greatest ecological pressure and the most severe water shortage  
69 in China. The purpose of this study is to: (1) analyze the SPAC water cycle process in different  
70 vegetation areas and (2) identify the potential factors that control the SPAC water cycle. The research is  
71 helpful to clarify the water resource utilization mechanism and the local water cycle mechanism of  
72 different vegetation areas in high mountainous areas and provides a specific theoretical basis and  
73 guiding suggestions for the practical and reasonable use of water resources in arid areas.

## 74 **2 Materials and methods**

### 75 **2.1 Study area**

76 The Shiyang River Basin is located at the northern foot of the Qilian Mountains, east of the Hexi  
77 Region, Gansu Province (Zhu et al., 2018) (Fig. 1). The Shiyang River originates from the  
78 snow-capped mountains on the north side of the Lenglongling in the eastern section of the Qilian  
79 Mountains. The river's total length is about 250 km, with a basin area of  $4.16 \times 10^4 \text{ km}^2$ , and the annual  
80 average runoff is about  $1.58 \times 10^8 \text{ km}^3$ . River supplies come from meteoric mountain precipitation and  
81 alpine ice and snow melt water. The runoff area is about  $1.10 \times 10^4 \text{ km}^2$ , and the drought index is 1 to 4  
82 (Zhou et al., 2020). The soil is classified as grey brown desert soil, aeolian sandy soil, saline soil, and  
83 meadow soil. The Shiyang River Basin has a continental temperate arid climate with strong sunlight.  
84 The annual average sunshine hours are 2604.8-3081.8 hours, the annual average temperature is

85 -8.2-10.5°C, the temperature difference between day and night is 25.2°C, the annual average  
86 precipitation is 222 mm, and the annual average evaporation is 700-2000 mm. The vegetation coverage  
87 in the upper and middle alpine regions is better than that of the lower reaches, with trees, shrubs, and  
88 grass covered (Wan et al., 2019). The downstream vegetation coverage is poor under the strong  
89 influence of long-term human production and life, mainly desert vegetation.

90 **Fig 1** about here

## 91 **2.2 Sample collection**

92 From April 2018 to October 2019, samples were collected at Lenglong (alpine meadow), Hulin  
93 (forest), and Xiyang (arid foothills) in the Shiyang River Basin (Table 1). We collected 1281 samples in  
94 the Shiyang River Basin, including 472 precipitation samples, 570 soil samples, 119 plant samples, and  
95 120 groundwater samples.

96 **Table 1** about here

97 The precipitation samples are collected with a rain bucket. The rain measuring cylinder consists of  
98 a funnel and a storage part. After each precipitation event, the collected liquid precipitation is  
99 immediately transferred to a 100 ml high-density sample bottle. The sample bottle is sealed with a  
100 sealing film and stored at low temperature. Simultaneously, the polyethylene bottle sample is labeled  
101 with the date and type of precipitation (rain, snow, hail, and rain).

102 The soil samples are collected at intervals of 10 cm at a depth of 100 cm with a soil drill. Part of  
103 the soil sample were put into a 50 ml glass bottle. The bottle's mouth was sealed with parafilm and  
104 transported to the observation station for cryopreservation within 10 hours after sampling. The  
105 remaining soil sample was placed in a 50 ml aluminum box and used the drying method to measure the  
106 soil water content (swc).

107 The vegetation samples are collected with a sampling shear. First, we peel off the bark and put the  
108 stem into a 50 ml glass bottle. After that, we sealed the bottle mouth and keep it frozen before the  
109 experimental analysis.

110 The groundwater was collected with polyethylene bottles, and the samples were brought back to

111 the refrigerator at the test station for cryogenic preservation within 10 hours.

## 112 2.3 Sample treatment

113 All water samples are tested using a liquid water analyzer (DLT-100, Los Gatos Research Center,  
114 USA) in the Northwest Normal University laboratory. Each sample and isotope standard was analyzed  
115 by six consecutive injections. To eliminate the memory effect of the analyzer, we discarded the values  
116 of the first two injections and used the average of the last four injections as the final result value.

117 Isotopic measurements are given with the symbol "δ" and are expressed as a difference of thousandths  
118 relative to Vienna Standard Mean Ocean Water:

$$119 \quad \delta (\text{‰}) = [(\delta/\delta_{v-smow}) - 1] \times 1000 \quad (1-1)$$

120 Where, δ is the ratio of <sup>18</sup>O/<sup>16</sup>O or <sup>D</sup>/<sup>1</sup>H in the collected sample, δ<sub>v-smow</sub> is the ratio of <sup>18</sup>O/<sup>16</sup>O or  
121 <sup>D</sup>/<sup>1</sup>H in the Vienna standard sample.

122 Due to the existence of methanol and ethanol in plant water samples, it is necessary to calibrate  
123 the original data of plant samples. Using different concentrations of pure methanol and ethanol mixed  
124 deionized water, combined with Los Gatos' LWIA-spectral pollutant identification instrument V1.0  
125 spectral analysis software, the establishment of δD and δ<sup>18</sup>O spectral pollutant correction method,  
126 determine methanol (NB) and ethanol (BB) pollution degree (Meng et al., 2012; Liu et al., 2015). For  
127 the broadband metric value NB metric of the methanol calibration result, its logarithm has a significant  
128 quadratic curve relationship with ΔδD and Δδ<sup>18</sup>O, and the formulas are respectively:

$$129 \quad \Delta\delta D = 0.018 (\ln NB)^3 + 0.092 (\ln NB)^2 + 0.388 \ln NB + 0.785 \quad (R^2 = 0.991, p < 0.0001) \quad (2-1)$$

$$130 \quad \Delta\delta^{18}O = 0.017 (\ln NB)^3 - 0.017 (\ln NB)^2 + 0.545 \ln NB + 1.358 \quad (R^2 = 0.998, p < 0.0001) \quad (2-2)$$

131 For ethanol calibration results, the broadband metric value BB metric has a quadratic curve and a  
132 linear relationship with ΔδD and Δδ<sup>18</sup>O, and the formulas are respectively:

$$133 \quad \Delta\delta D = -85.67 BB + 93.664 \quad (R^2 = 0.747, p = 0.026) \quad (BB < 1.2) \quad (2-3)$$

$$134 \quad \Delta\delta^{18}O = -21.421 BB^2 + 39.9356 \quad (R^2 = 0.769, p < 0.012) \quad (2-4)$$

## 135 2.4 Data analysis

136 Since the isotopic data are generally normally distributed according to the Kolmogorov-Smirnov  
137 (KS) test, we use Pearson correlation to describe the various correlations between different water types  
138 (precipitation, soil water, plant water, and groundwater) and the control factors in different vegetation

139 **zones**. The significance level for all statistical tests was set to the 95% confidence interval. All  
140 statistical analyses were performed using SPSS software.

### 141 **3. Results**

#### 142 **3.1 Changes in meteorological parameters over time**

143 **Figure 2 shows the changes in daily precipitation, relative humidity, temperature, and swc from**  
144 **April 2018 to October 2019. Meteorological data are obtained from the meteorological station in the**  
145 **Shiyang River Basin.** During the summer monsoon (April to September), the accumulated precipitation  
146 accounts for 90.4% of the total precipitation, and the average daily precipitation was 3.98 mm. During  
147 the winter monsoon (October to March), the accumulated precipitation accounts for 9.60% of the total  
148 precipitation, with an average daily precipitation of 0.13 mm. During the summer monsoon, the relative  
149 humidity in the Shiyang River Basin was 43.78%, while **during the winter monsoon it was 35.78%.**  
150 During the observation period, the temperature between -16.2°C and 32°C, and the average temperature  
151 of summer monsoon and winter monsoon were 20.20°C and -0.69°C, respectively. The average SWC  
152 value of 0-100cm soil layer varies from 2.58% to 89.96 %, and the low SWC value usually appears in  
153 summer, **which relates to the strong soil evaporation.**

154

**Fig 2** about here

#### 155 **3.2 The relationship between water stable isotopes in different vegetation zones**

156 According to the definition of the global meteoric water line (GMWL) (Craig, 1961), the linear  
157 relationship of  $\delta^{18}\text{O}$  and  $\delta\text{D}$  in local precipitation, soil water, plant water, and groundwater is defined as  
158 LMWL, SWL, PWL, and GWL, respectively.

159 As shown in Fig. 3, there are some differences in the atmospheric waterline equations of different  
160 vegetation zones. The **slope of** LMWL of alpine meadows (7.88), forests (7.82), and arid foothills (7.72)  
161 is all smaller than that of GMWL (8.00), this is because the study area is located in northwestern  
162 China's arid area, the climate is dry, and the isotopes have undergone strong fractionation. The slope of  
163 the SWL in the alpine meadow is the largest (6.07), and the slope of the SWL in the forest (5.10) is  
164 greater than the slope of the SWL in the arid foothills (3.94), the intercept has the same characteristics,  
165 indicating that the arid foothills' soil evaporation is the largest. According to the Natural Resources  
166 Survey Report of the Shiyang River Basin in 2020, the vegetation coverage rate of the alpine meadow  
167 is 25.95%, and that of the arid foothills is 8.48%. The vegetation coverage rate of the alpine meadow is

168 higher than that of the arid foothills, with better water retention ability and less evaporation of soil  
169 water (Wan et al., 2019; Wei et al., 2019). The slope of the PWL in the arid foothills is the largest  
170 (2.45), and the slope of the PWL in the alpine meadow (1.90) is greater than that of the forest (1.69).

171 According to the weighted average value of stable oxygen isotopes of various water bodies (Table  
172 2), alpine meadows' soil water  $\delta^{18}\text{O}$  is -9.16‰, the most depleted and the closest to the precipitation  
173  $\delta^{18}\text{O}$  (-9.44‰). The average  $\delta^{18}\text{O}$  of groundwater is -8.84‰, which is between  $\delta^{18}\text{O}$  of plant (-1.68‰)  
174 and  $\delta^{18}\text{O}$  of precipitation (-9.44‰), indicating that precipitation is the primary source of alpine  
175 meadows replenishment. The precipitation  $\delta^{18}\text{O}$  of the forest (-7.50‰) is the most depleted, and the  
176 average  $\delta^{18}\text{O}$  of groundwater (-8.56‰) is between soil water  $\delta^{18}\text{O}$  (-7.01‰) and precipitation  $\delta^{18}\text{O}$   
177 (-8.63‰), but it is close to precipitation  $\delta^{18}\text{O}$ , indicating that forest groundwater is replenished by soil  
178 water and precipitation. The mean  $\delta^{18}\text{O}$  of soil water (-8.23‰) in the arid foothills are between  
179 precipitation  $\delta^{18}\text{O}$  (-7.50‰) and groundwater  $\delta^{18}\text{O}$  (-8.88‰) but closer to groundwater  $\delta^{18}\text{O}$ , indicating  
180 that the soil water in the arid foothills is mainly supplied by groundwater.

181

Fig 3 about here

182

Table 2 about here

### 183 3.3 Relationship between soil water and plant water isotope in different vegetation zones

184 By analyzing the isotopic composition of soil and plant xylem, it is possible to preliminarily  
185 determine whether there is an overlap between soil moisture and plant moisture at different depths  
186 (Javaux et al., 2016; Dawson et al., 1993; Rothfuss et al., 2017; Tetzlaff et al., 2017; McCole et al.,  
187 2007; Zhou et al., 2015; Schwendenmann et al., 2015). Soil water may evaporate before it is absorbed  
188 by plants, which leads to the increase of  $\delta\text{D}$  and  $\delta^{18}\text{O}$  values of soil water (Chen et al., 2014). Therefore,  
189 it can be well explained that the surface soil water isotope in Fig. 4 is more enriched than the deep soil  
190 water isotope.

191 According to the study area's precipitation, the current experiment is divided into the dry season  
192 (October-April of the following year) and the rainy season (May-September) for analysis (Fig. 4). In  
193 the dry season, alpine meadow plants have the highest value of  $\delta^{18}\text{O}$  (-2.84‰), and there is no overlap  
194 between soil and plant water. In the rainy season, the plant water  $\delta^{18}\text{O}$  (-6.04‰) and precipitation  $\delta^{18}\text{O}$

195 (-6.40‰) are close, **the groundwater and soil water's surface and deep layers intersect**, indicating that  
196 plant water is mainly supplied by precipitation in the rainy season, while the groundwater is supplied  
197 by soil water. In the dry season, due to the low temperature (average temperature 0.30°C), there is a lot  
198 of ice and snow in alpine meadows, and plants do not directly use soil water. As the increase of  
199 temperature (average temperature 8.72°C), precipitation and surface runoff increases, **and water**  
200 **infiltrate into groundwater from soil**. Forest plant water intersects with deep soil during the dry season  
201 and intersects with the soil surface during the rainy season, indicating that forest plants mainly use deep  
202 soil water during the dry season and shallow soil water during the rainy season. In the rainy season, the  
203 surface layer of soil water intersects with plant water, **the groundwater and soil water's surface and**  
204 **deep layers intersect**, showing that the plant water preferentially uses the surface layer water of the soil  
205 **in the arid foothills**. In the dry season, plant water **oxygen is the most enriched**, and the isotopic values  
206 of groundwater and soil water are close, **indicating** that the soil water is mainly recharged by the  
207 groundwater. According to the natural resources survey report of the Shiyang River Basin, the buried  
208 groundwater level **in the arid foothills** is 2.5-15 m, and the groundwater **table** is relatively shallow,  
209 making the soil water in the arid foothills mainly recharged by groundwater in the dry season.  
210

**Fig 4** about here

## 211 **4. Discussion**

### 212 **4.1 Variation of soil **water** isotope and SWC between different vegetation zones**

213 **In Fig. 5**, along the three vegetation zones of alpine meadow-forest-arid foothills, soil water  
214 isotope is gradually enriched. **The coefficient of variation of the arid foothills is the largest (-0.15),**  
215 **while that of the forest is the smallest (-0.25), indicating that from forest to arid foothills, the closer to**  
216 **arid regions, the greater the coefficient of variation and that the greater the instability of stable isotope**  
217 **soil water**. The soil water isotopes of different vegetation zones showed the same characteristics as the  
218 soil depth changed, that is, they were all depleted in May and August and enriched in October.

219 The **swc** of alpine meadows (average  $\theta$  of 42.21 %) is higher than that of forests (average  $\theta$  of  
220 26.98 %) and arid foothills (average  $\theta$  of 17.05 %), and the **swc** of alpine meadows increases with the  
221 increase of soil depth (from 43.78 % to 49.27 %), while that of forests the **swc** decreases with the soil  
222 depth (from 26.10 % to 25.41 %). Compared with forests, plants in alpine meadows have shallower root  
223 systems and smaller canopies, so transpiration and water consumption are lower, and **swc** is higher  
224 (Csilla et al., 2014; Li et al., 2009; Western et al., 1998). On the one hand, with the improvement of  
225 vegetation restoration, the ability to retain **soil** water in the alpine meadows has increased, and the  
226 amount of soil water evaporation has reduced. **On the other hand, Lenglong, a representative of alpine**  
227 **meadows, has an average annual precipitation of 595.10 mm, and a low temperature (average annual**  
228 **temperature of -0.20°C), makes the soil water evaporation intensity weak.** The **swc** of the alpine  
229 meadows (86.95 %) and forests (53.45 %) is the largest in August, while the arid foothills' **swc**  
230 (11.13 %) is the smallest in August, this is because the northern slope of the Qilian Mountains is a  
231 windward slope. **In August, a lot of precipitation falls on the high-altitude alpine meadows and forests,**  
232 **the arid foothills have little precipitation and low swc.**  
233

Fig 5 about here

## 234 4.2 Control factors of SPAC in different vegetation zones

### 235 4.2.1 The influence of temperature on SPAC

236

As shown in Fig. 6, with the changes in the water cycle of precipitation-soil water-plant water, the  
237  $\delta^{18}\text{O}$  of forests gradually accumulates, while the soil water  $\delta^{18}\text{O}$  of arid foothills and alpine meadows  
238 are the most depleted in summer. In other seasons,  $\delta^{18}\text{O}$  is gradually enriched along with  
239 precipitation-soil water-plant water. In summer, there is much precipitation and large **swc** in alpine  
240 meadows, but due to low temperature (average temperature in summer is 9.80°C), the soil water  $\delta^{18}\text{O}$   
241 of alpine meadows is relatively depleted. In the arid foothills, in summer, especially in August,  
242 although the temperature is relatively high (the average temperature is 23.92°C), the **swc** is low,  
243 evaporation is weak, and  $\delta^{18}\text{O}$  are relatively depleted. This phenomenon shows that precipitation plays  
244 a major control role in the water cycle of precipitation-soil-plants. **When** the temperature is below 0°C,

245 the air will expand adiabatically, and the water vapor will change adiabatic cooling (Rozanski, 1992).  
246 When the temperature is between 0°C and 8°C, the influence of local water vapor circulation is greater.  
247 When the temperature is below 8°C, the below-cloud evaporation is very strong (Zhu et al., 2021).  
248 Therefore, we divided the temperature into three gradients (below 0°C, between 0°C and 8°C and  
249 above 8°C) for analysis. From the alpine meadow to arid foothills, the correlations between  
250 temperature and soil  $\delta^{18}\text{O}$  are 0.41, 0.30, and 0.19, respectively, and the correlations with plant  $\delta^{18}\text{O}$  are  
251 0.24, 0.27, and 0.25, respectively, and the temperature effect is not significant compared with  
252 precipitation. As shown in Table 3, from the alpine meadow to the arid foothills, the temperature effect  
253 of the precipitation isotope is enhanced, and there is a significant positive correlation with temperature,  
254 and all have passed the significance test. With the increase of temperature, the temperature effect and  
255 the linear relationship of precipitation isotope in each vegetation area weakened. When the temperature  
256 is lower than 0°C, the correlation between precipitation  $\delta^{18}\text{O}$  and the temperature in the arid foothills  
257 fails the significance test. The relationship between  $\delta^{18}\text{O}$  and temperature in alpine meadows, forests,  
258 and arid foothills are  $\delta^{18}\text{O}=0.62T-10.84$ ,  $\delta^{18}\text{O}=1.58T-12.14$ , and  $\delta^{18}\text{O}=1.29T-11.78$ , respectively. When  
259 the temperature is between 0°C and 8°C, as the temperature increases, the temperature effect of  
260 precipitation weakens, which may be related to the weakening of the local water cycle and the  
261 enrichment of precipitation isotopes. The relationship between  $\delta^{18}\text{O}$  and temperature in alpine  
262 meadows, forests, and arid foothills are  $\delta^{18}\text{O}=0.51T-11.41$ ,  $\delta^{18}\text{O}=2.46T-22.84$ , and  $\delta^{18}\text{O}=2.27T-22.78$ ,  
263 respectively. When the temperature is above 8°C, there is no correlation between the precipitation  $\delta^{18}\text{O}$   
264 and the temperature, but the precipitation  $\delta^{18}\text{O}$  is the most enriched, which may be related to the  $\delta^{18}\text{O}$   
265 enrichment caused by the below-cloud evaporation. The relationship between  $\delta^{18}\text{O}$  and temperature in

266 alpine meadows, forests, and arid foothills are  $\delta^{18}\text{O}=0.48T-10.82$ ,  $\delta^{18}\text{O}=0.13T-7.76$ , and  
267  $\delta^{18}\text{O}=0.27T-10.13$ , respectively.

268 **Fig 6** about here

269 **Table 3** about here

#### 270 4.2.2 The influence of altitude on SPAC

271 In Fig.7, the altitude effect of precipitation  $\delta^{18}\text{O}$  is the strongest, and the relationship between  
272 plant water  $\delta^{18}\text{O}$  and altitude is weakest, showing that in SPAC, precipitation isotope is most affected  
273 by altitude, and plant water isotope is least affected by altitude. From the arid foothills to alpine  
274 meadows, the elevation rises from 2097m to 3647m, and the change rate of  $\delta^{18}\text{O}$  and  $\delta\text{D}$  were  $-0.11\%$   
275  $(100\text{m})^{-1}$  and  $-0.41\%$   $(100\text{m})^{-1}$ . As the water vapor quality rises along the hillside, the temperature  
276 continues to decline, and the isotopic values of precipitation continue to consume. In the rainy season,  
277 the squares of the correlation coefficients between  $\delta^{18}\text{O}$  and  $\delta\text{D}$  of precipitation and altitude are 0.79  
278 and 0.98, the change rate of  $\delta^{18}\text{O}$  and  $\delta\text{D}$  are  $-0.12\%$   $(100\text{m})^{-1}$  and  $-1.05\%$   $(100\text{m})^{-1}$ , respectively. In  
279 the dry season, the correlation coefficient squares of  $\delta^{18}\text{O}$  and  $\delta\text{D}$  with altitude are 0.88 and 0.90,  
280 respectively, and the rate of  $\delta^{18}\text{O}$  and  $\delta\text{D}$  change is  $-0.18\%$   $(100\text{m})^{-1}$  and  $-0.79\%$   $(100\text{m})^{-1}$ , respectively.  
281 We can see that the altitude effect of precipitation  $\delta^{18}\text{O}$  is stronger in the dry season ( $R^2=0.88$ ) than in  
282 the rainy season ( $R^2=0.79$ ). The results showed that as the temperature increase, the temperature effect  
283 of precipitation  $\delta^{18}\text{O}$  masks the altitude effect, which leads to the weakening of the altitude effect of  
284 precipitation  $\delta^{18}\text{O}$ . The relationship between soil water  $\delta^{18}\text{O}$  and altitude is stronger in the dry season  
285 ( $R^2=0.26$ ) than in the rain season ( $R^2=0.28$ ). The relationship between plant water  $\delta^{18}\text{O}$  and altitude is  
286 stronger in the dry season ( $R^2=0.11$ ) than in the rainy season ( $R^2=0.10$ ), this is consistent with the  
287 changes in the altitude effect of precipitation isotope which is related to precipitation playing a major

288

controlling role in SPAC.

289

Fig 7 about here

290

#### 4.2.3 The influence of relative humidity and precipitation on SPAC

291

292

To find out the potential factors that control the isotope composition of SPAC in different vegetation zones, we also analyzed the influence of relative humidity and precipitation on  $\delta^{18}\text{O}$  of

293

SPAC. It can be seen from Fig. 8 and Table 4 that the greatest impact of relative humidity on the

294

isotope composition of SPAC appears in the arid foothills in the dry season, with a correlation

295

coefficient of 0.38. In the dry season, the square of the correlation coefficient between forest

296

precipitation isotope and relative humidity Although it is 0.78, there is an inverse humidity relationship

297

between the two, which may be related to the lack of precipitation samples in the dry season. The

298

largest impact of precipitation on the isotopic composition of SPAC occurs in the arid foothills in the

299

rainy season, and the square of the correlation coefficient is 0.14. It can also be seen from Figure 8 that

300

the influence of relative humidity and precipitation have a greater influence on precipitation isotope

301

than that of plant water isotope and soil water isotope. The influence of relative humidity and

302

precipitation on the isotopic composition of SPAC in alpine meadows is greater than that of arid

303

foothills and greater than that of forests. In general, the SPAC isotopic composition of alpine meadows,

304

forests, and arid foothills has a weak precipitation effect, and the correlation with relative humidity is

305

also weak.

306

By comparing the correlation of temperature, altitude, relative humidity and precipitation with

307

SPAC isotope composition in different vegetation zones, we can see that the correlation between

308

temperature and altitude and SPAC isotope composition is stronger than relative humidity and

309

precipitation. Temperature and altitude are potential factors that control the isotope composition of

310

SPAC. However, in the dry season, there is a phenomenon that the temperature effect conceals the altitude effect.

312

**Fig 8** about here

313

**Table 4** about here

## 314 **5. Conclusion**

315 This paper uses the hydrogen and oxygen isotope method to study the differences and control  
316 factors of SPAC in different vegetation zones. Temperature and altitude are the main controlling factors  
317 for the isotope composition of SPAC. From alpine meadows to forests to arid foothills, as the decreases  
318 of altitude, the temperature effect of precipitation isotope increases, and the influence of temperature  
319 also increases. When the temperature is lower than 0°C, the temperature effect of the vegetation zone is  
320 the strongest. In the dry season, there is a phenomenon that the temperature effect masks the altitude  
321 effect. With the increase of the soil depth, the soil water isotopes are gradually depleted. The soil water  
322 content of alpine meadows is the largest and increases with the soil depth, while the soil water content  
323 in forest decreases with the soil depth, and the soil water content of the arid foothills is the least in  
324 August. In the rainy season, plants mainly use precipitation, while in the dry season, forest plants  
325 mainly use soil water, while alpine meadow plants do not directly use soil water because of the  
326 abundant precipitation and melt water in the growing season. Exposure to the groundwater table in the  
327 arid foothills can provide water for plants in the dry season. Because forests and grasslands affect  
328 intercepting rainfall, they delay or hinder the formation of surface runoff and convert part of the surface  
329 runoff into soil flow and groundwater, which can provide part of water resources for plants. To better  
330 understand the water cycle of SPAC at different temperatures and altitudes in high mountain areas,  
331 long-term observations of different plants are needed to provide a theoretical basis for the rational and  
332 practical use of water resources in arid mountainous areas.

## 333 **Data Availability**

334 The data that support the findings of this study are openly available in Zhu (2021), "Stable  
335 water isotope monitoring network of different water bodies in Shiyang River Basin, a typical arid  
336 river in China (Supplemental Edition 20210808)", Mendeley Data, V1, doi:  
337 10.17632/d5kzm92nn3.1.

338 **Author contribution**

339 Guofeng Zhu and Yuwei Liu conceived the idea of the study; Zhuaxia Zhang analyzed the data;  
340 Zhigang Sun and Leilei Yong were responsible for field sampling; Liyuan Sang participated in the  
341 experiment; Kailiang Zhao participated in the drawing; Yuwei Liu wrote the paper; Liyuan Sang and  
342 Lei Wang checked and edited language. All authors discussed the results and revised the manuscript.

343 **Competing interests**

344 The authors declare no competing interests

345 **Acknowledgments**

346 This research was financially supported by the National Natural Science Foundation of China  
347 (41661005, 41867030, 41971036). The authors much thank the colleagues in the Northwest Normal  
348 University for their help in fieldwork, laboratory analysis, data processing.

349 **References**

- 350 Araguás-Araguás, L., Froehlich, K., and Rozanski, K.: Stable isotope composition of precipitation over  
351 southeast asia. *Journal of Geophysical Research Atmospheres*, 103 (D22), 28721-28742, doi:  
352 10.1029/98JD02582,1998.
- 353 Bam, E., and Ireson, A. M.: Quantifying the wetland water balance: a new isotope-based approach that  
354 includes precipitation and infiltration. *Journal of Hydrology*, 570, doi:  
355 10.1016/j.jhydrol.2018.12.032, 2018.
- 356 Chen, X. L., Chen, Y. N., and Chen, Y. N P.: Water use relationship of desert riparian forest in lower  
357 reaches of Heihe River. *Chinese Journal of Eco-Agriculture*, 22 (08):972-979,  
358 doi:10.1007/s11430-013-4680-8, 2014.
- 359 Christopher, T., Solomon, J. J., and Cole.: *The influence of environmental water on the hydrogen stable*  
360 *isotope ratio in aquatic consumers. Oecologia*, 161 (2), p.313-324, doi:  
361 10.1007/s00442-009-1370-5, 2009.
- 362 Coenders-Gerrits, A. M. J., van der Ent, R.J., Bogaard, T. A., Wang-Erlandsson, L., Hrachowitz, M.,  
363 Savenije, and H. H. G.: Uncertainties in transpiration estimates. *Nature*. 506, E1–E2, doi:  
364 10.1038/nature12925, 2014.
- 365 Coplen, T.: Stable isotope hydrology: deuterium and oxygen 18 in the water cycle. *Eos Transactions*  
366 *American Geophysical Union*, 63 (45), 861-862, doi: 10.1029/EO063i045p00861, 2013.
- 367 Cortes, A., and Farvolden, R. N.: Isotope studied of precipitation and groundwater in the sierra de las

368 cruces, Mexico. *Journal of Hydrology*, 107 (1–4), 147-153, doi:  
369 10.1016/0022-1694(89)90055-3,1989.

370 Craig, H.: Isotopic variations in meteoric water. *Science*, 133, 1702–1703, doi:  
371 10.1126/science.133.3465.1702,1961.

372 Csilla, F., Györgyi, G., Zsófia, B., and Eszter, T.: Impact of expected climate change on soil water  
373 regime under different vegetation conditions. *Biologia*, doi: 10.2478/s11756-014-0463-8, 2014.

374 Dai, J. J., Zhang, X. P., Luo, Z. D., Wang, R., Liu, Z. L., He, X. G., and Guan, H. D.: Variation of the  
375 stable isotopes of water in the soil-plant-atmosphere continuum of a *Cinnamomum camphora*  
376 woodland in the East Asian monsoon region. *Journal of Hydrology*, 589, 125199. doi:  
377 10.1016/J.JHYDROL.2020.1251, 2020.

378 Darling, W. G. , Bath, A. H. , and Talbot, J. C.: The O and H stable isotope composition of freshwaters  
379 in the british isles. 2, surface waters and groundwater. *Hydrology and Earth System Sciences*, doi:  
380 10.5194/hess-7-183-2003, 2003.

381 Dawson, T. E., and Ehleringer, J. R.: Streamside trees that do not use stream water. *Nature*, 350 (6316),  
382 335-337, doi: 10.1038/350335a0, 1991.

383 Dawson, T. E.: Water sources of plants as determined from xylem-water isotopic composition:  
384 perspectives on plant competition, distribution, and water relations stable isotopes and plant  
385 carbon water relations. *Stable Isotopes and Plant Carbon-water Relations*, 465-496, 1993.

386 Detjen, M., Sterling, E. , and Gómez, A.: Stable isotopes in barnacles as a tool to understand green sea  
387 turtle (*Chelonia mydas*) regional movement patterns. *Biogeosciences*, 2015.

388 Durand, J. L., Bariac, T., M Ghesquière, Biron, P., Richard, P., and Humphreys, M.: Ranking of the  
389 depth of water extraction by individual grass plants, using natural <sup>18</sup>O isotope  
390 abundance. *Environmental and Experimental Botany*, 60 (1), 137-144, doi:  
391 10.1016/j.envexpbot.2006.09.004, 2007.

392 Ehleringer, L.: Stable isotope composition of stem and leaf water: applications to the study of plant  
393 water use. *Functional Ecology*, 5 (2), 270-277, doi:10.2307/2389264,1991.

394 Gao, J., Tian, L. D., Liu, Y. Q., and Gong, T. L.: Oxygen isotope variation in the water cycle of the  
395 yamzho lake basin in southern tibetan plateau. *Chinese Science Bulletin*, (16), 2758-2765, 2009.

396 Gao, J., Yao, T., Tian, L.D., Risi, C., and Hoffmann, G.: Precipitation water stable isotopes in the south  
397 tibetan plateau: observations and modeling. *Journal of Climate*, 24 (13), 3161-3178, doi:

398 10.1175/2010JCLI3736.1, 2011.

399 Hou, S. B., Song, X. F., Jie, Y. J., Liu, X., and Zhang, G. Y.: Stable isotopes characters in the process of  
400 precipitation and infiltration in taihang mountainous region. *Resources Science*, 2008.

401 Hua, M. Q., Zhang, X. P., Yao, T. C., and He, X. G.: Dual effects of precipitation and evaporation on  
402 lake water stable isotope composition in the monsoon region. *Hydrological Processes*, 33,  
403 2192–2205, doi: 10.1002/hyp.13462, 2019.

404 Jasechko, S., Sharp, Z. D., Gibson, J. J., Birkes, S. J., Yi, Y., and Fawcett, P. J.: Terrestrial water fluxes  
405 dominated by transpiration. *Nature*, 496 (7445), 347–351, doi: 10.1038/nature11983, 2013.

406 Javaux, M., Rothfuss, Y., Vanderborght, J., Vereecken, H., and Brüggemann, N.: Isotopic composition  
407 of plant water sources. *Nature*, 536 (7617), E1–E3, doi: 10.1038/nature18946, 2016.

408 Li, C. C., Huang, M. S., Liu, J., Ji, S. P., and Zhao, R. Q.: Isotope-based water-use efficiency of major  
409 greening plants in a sponge city in northern China. *PloS one*, 14 (7), doi:  
410 10.1371/journal.pone.0220083, 2019.

411 Li, L. F., Yan, J. P., Liu, D. M., Chen, F., and Ding, J. M.: Changes in soil water content under different  
412 vegetation conditions in arid-semi-arid areas and analysis of vegetation construction methods.  
413 *Bulletin of Soil and Water Conservation*, 29 (001), 18-22, 2009.

414 Li, S. G., Maki, T., Atsuko, S., and Michiaki, S.: Seasonal variation in oxygen isotope composition of  
415 waters for a montane larch forest in Mongolia. *Trees* (1), doi: 10.1007/s00468-005-0019-1, 2006.

416 Liu, W., Wang, P., Li, J., Liu, W., and Li, H.: Plasticity of source-water acquisition in epiphytic,  
417 transitional and terrestrial growth phases of *Ficus tinctoria*. *Ecohydrology*, 7 (6), 1524–1533, doi:  
418 10.1002/eco.1475, 2015.

419 McCole, A. A., and Stern, L. A.: Seasonal water use patterns of *Juniperus ashei* on the Edwards Plateau,  
420 Texas, based on stable isotopes in water. *Journal of Hydrology*, 342, 238–248, doi:  
421 10.1016/j.jhydrol.2007.05.024, 2007.

422 Meissner, K., Schwendenmann, H., and Dyckmans.: Soil water uptake by trees using water stable  
423 isotopes ( $\delta D$  and  $\delta^{18}O$ )- a method test regarding soil moisture, texture and carbonate. *Plant*  
424 *Soil*, 376, 327-335, doi: 10.1007/s11104-013-1970-z, 2014.

425 Meng, X. Q., Wen, X. F., Zhang, X. Y., Han, J. Y., Sun, X. M., and Li, X. B.: Influence of organics on  
426 the determination of  $\delta^{18}O$  and  $\delta D$  of plant leaves and stalk water by infrared spectroscopy, *Chin J*  
427 *Eco-agri*, 20, 1359-1365, 2012.

428 Nie, Y. P., Chen, H. S., Wang, K. L., and Ding, Y. L.: Rooting characteristics of two widely distributed  
429 woody plant species growing in different karst habitats of southwest China. *Plant Ecol*, 215  
430 (10),1099-1109, doi: 10.1007/s11258-014-0369-0, 2014.

431 Nlend, B., Celle-Jeanton, H., Risi, C., Pohl, B., and Ketchemen-Tandia, B.: Identification of processes  
432 that control the stable isotope composition of rainwater in the humid tropical west-central  
433 Africa. *Journal of Hydrology*, 584, 124650, doi:10.1016/j.jhydrol.2020.124650, 2020.

434 Porporato, L.: Plants in water-controlled ecosystems: active role in hydrologic processes and response  
435 to water stress. *Advances in Water Resources*, 24 (7), 725-744, doi:  
436 10.1016/S0309-1708(01)00005-7, 2001.

437 Price, R. M., Skrzypek, G., Grierson, P. F., Swart, P. K., and Fourqurean, J. W.: The use of stable  
438 isotopes of oxygen and hydrogen to identify water sources in two hypersaline estuaries with  
439 different hydrologic regimes. *Marine and Freshwater Research*, 63 (11), 952-966. doi:  
440 10.1071/MF12042, 2012.

441 Raco, B., Dotsika, E., Feroni, A. C., Battaglini, R., and Poutoukis, D.: Stable isotope composition of  
442 italian bottled waters. *Journal of Geochemical Exploration*, 124, doi:  
443 10.1016/j.gexplo.2012.10.003, 2013.

444 Rothfuss, Y., and Javaux, M.: Reviews and syntheses: Isotopic approaches to quantify root water  
445 uptake: A review and comparison of methods. *Biogeosciences*, 14, 2199,  
446 doi:10.5194/bg-14-2199-2017, 2017.

447 Rozanski, K., Araguas-Araguas, L., and Gonfiantini, R.: Relation between long-term trends of  
448 oxygen-18 isotope composition of precipitation and climate. *Science* 258 (5084), 981–985, doi:  
449 10.1126/science.258.5084.981, 1992.

450 Schlesinger, W. H., and Jasechko, S.: Transpiration in the global water cycle. *Agric Forest Meteorol*,  
451 180–190, 115–117, doi: 10.1016/j.agrformet.2014.01.011, 2014.

452 Schwendenmann, L., Pendall, E., Sanchez-Bragado, R., Kunert, N., Hölscher, D.: Tree water uptake in  
453 a tropical plantation varying in tree diversity: Interspecific differences, seasonal shifts and  
454 complementarity. *Ecohydrology*, 8 (1), 1–12, doi: 10.1002/eco.1479, 2015.

455 Shou, W. K., Hu, F. L., Alamusa., and Liu, Z. M.: Methods for studying water cycle and water sources  
456 in arid regions based on spac system. *Chinese Journal of Ecology*, 32 (8), 2194-2202, 2013.

457 Smith, G. I., Friedman, I., Gleason, J. D., and Warden, A.: Stable isotope composition of waters in

458       southeastern California: 2. groundwaters and their relation to modern precipitation. *Journal of*  
459       *Geophysical Research Atmospheres*, 97, doi: 10.1029/92JD00183,1992.

460       Song, X. F., Xia, J., Yu, J. J., and Liu, C. M.: Application of environmental isotope techniques to study  
461       the hydrological cycle mechanism of typical watersheds in North China. *Advances in*  
462       *Geographical Sciences*, 21 (6), 527-537, 2002.

463       Song, X., Barbour, M. M., Farquhar, G. D., Vann, D. R., and Helliker, B. R.: Transpiration rate relates  
464       to within and across species variations in effective path length in a leaf water model of oxygen  
465       isotope enrichment. *Plant, Cell and Environment*, 36 (7), 2013.

466       Sun, S. F., Huang, J. H., Lin, G. H., Zhao, W., and Han, X. G.: Application of stable isotope technique  
467       in the study of plant water use. *Acta Ecologica Sinica*, 25 (9), 2362-2371. Tech. Pap, No. 96 (48  
468       pp.), doi: 10.1360/982004-755, 2005.

469       Tetzlaff, D., Sprenger, M., and Soulsby, C.: Soil water stable isotopes reveal evaporation dynamics at  
470       the soil-plant-atmosphere interface of the critical zone. *Hydrol. Earth Syst. Sci*, 21, 3839–3858,  
471       2017.

472       Wan, Q. Z., Zhu, G. F., Guo, H. W., Zhang, Y., Pan, H. X., and Yong, L. L.: Influence of vegetation  
473       coverage and climate environment on soil organic carbon in the Qilian mountains. *Scientific*  
474       *Reports*, 9(1), 17623. doi: 10.1038/s41598-019-53837-4, 2019.

475       Wang, S.Y., Wang, Q. L., Wu, J. K., He, X. B., and Wang, L. H.: Characteristics of stable isotopes in  
476       precipitation and moisture sources in the headwaters of the Yangtze River. *Environmental*  
477       *Sciences*, 40 (6), 2615-2623, doi: 10.13227/j.hjlx.201811140, 2019.

478       West, A. G., Patrickson, S. J., and Ehleringer, J. R. : Water extraction times for plant and soil materials  
479       used in stable isotope analysis. *Rapid Communications in Mass Spectrometry*, 20 (8), 1317-1321.  
480       doi: 10.1002/rcm.2456, 2010.

481       Western, A. W., and Grayson, R. B.: The tarrawarra data set: soil moisture patterns, soil characteristics,  
482       and hydrological flux measurements. *Water Resources Research*, 34 (10), 2765-2768. doi:  
483       10.1029/98WR01833, 1998.

484       White, J., Cook, E., Lawrence, J. R., and Broecker, W. S.: The D/H ratios of sap in trees: implications  
485       for water sources and tree ring D/H ratios. *Geochim. Cosmochim. Acta*, 49 (1), 237–246, doi:  
486       10.1016/0016-7037(85)90207-8,1985.

487       Yang, B., Wen, X., and Sun, X.: Seasonal variations in depth of water uptake for a subtropical

488 coniferous plantation subjected to drought in an east asian monsoon region. *Agricultural and*  
489 *Forest Meteorology*, 201, 218-228, doi: 10.1016/j.agrformet.2014.11.020, 2015.

490 Yu, J. J., Song, X. F., Liu, X. C., Yang, C., Tang, C. Y., and Li, F. D.: A study of groundwater cycle in  
491 yongding river basin by using  $\delta D$ ,  $\delta^{18}O$  and hydrochemical data. *Journal of Natural Resources*,  
492 (03), 415-423, 2007.

493 Zhou, H., Zhao, W. Z., Zheng, X. J., and Li, S. J.: Root distribution of *Nitraria sibirica* with seasonally  
494 varying water sources in a desert habitat. *J. Plant Res*, 128, 613–622, 2015.

495 Zhou, J. J., Zhao, Y. R., Huang, P., and Liu, C. F.: Impacts of ecological restoration projects on the  
496 ecosystem carbon storage of inland river basin in arid area, China. *Ecological Indicators*, doi:  
497 10.1016/j.ecolind.2020.106803, 2020.

498 Zhu, G. F., Guo, H.W., Qin, D. H., Pan, H. X., and Ma, X. G.: Contribution of recycled moisture to  
499 precipitation in the monsoon marginal zone: estimate based on stable isotope data. *Journal of*  
500 *Hydrology*, 569, doi: 10.1016/j.jhydrol.2018.12.014, 2018.

501 Zhu, G. F., Zhang, Z. X., Guo H. W., Zhang, Y., Yong, L. L., Wan, Q. Z., Sun, Z. G., and Ma, H.Y.:  
502 Below-Cloud Evaporation of Precipitation Isotope over Mountain-oasis-desert in Arid Area. *Journ*  
503 *al of Hydrometeorology*, 22 (10): 2533-2545, doi: 10.1175/JHM-D-20-0170.1, 2021.

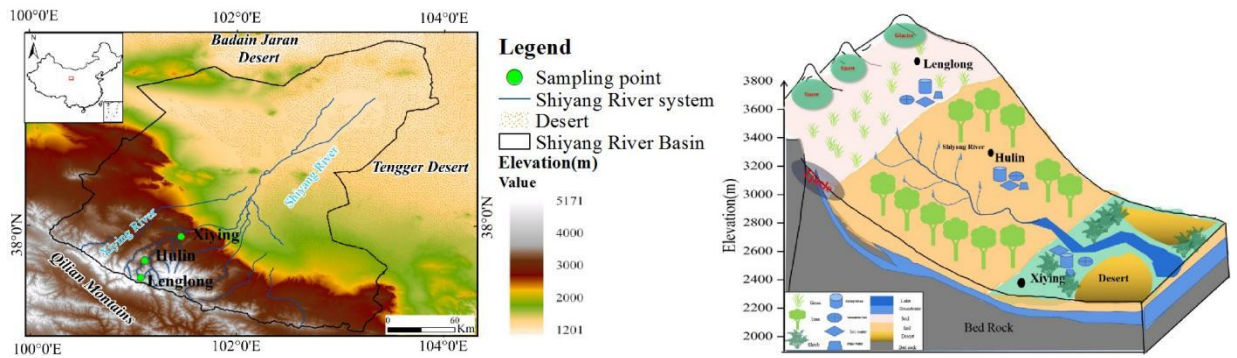


Fig. 1 Study area and observation system

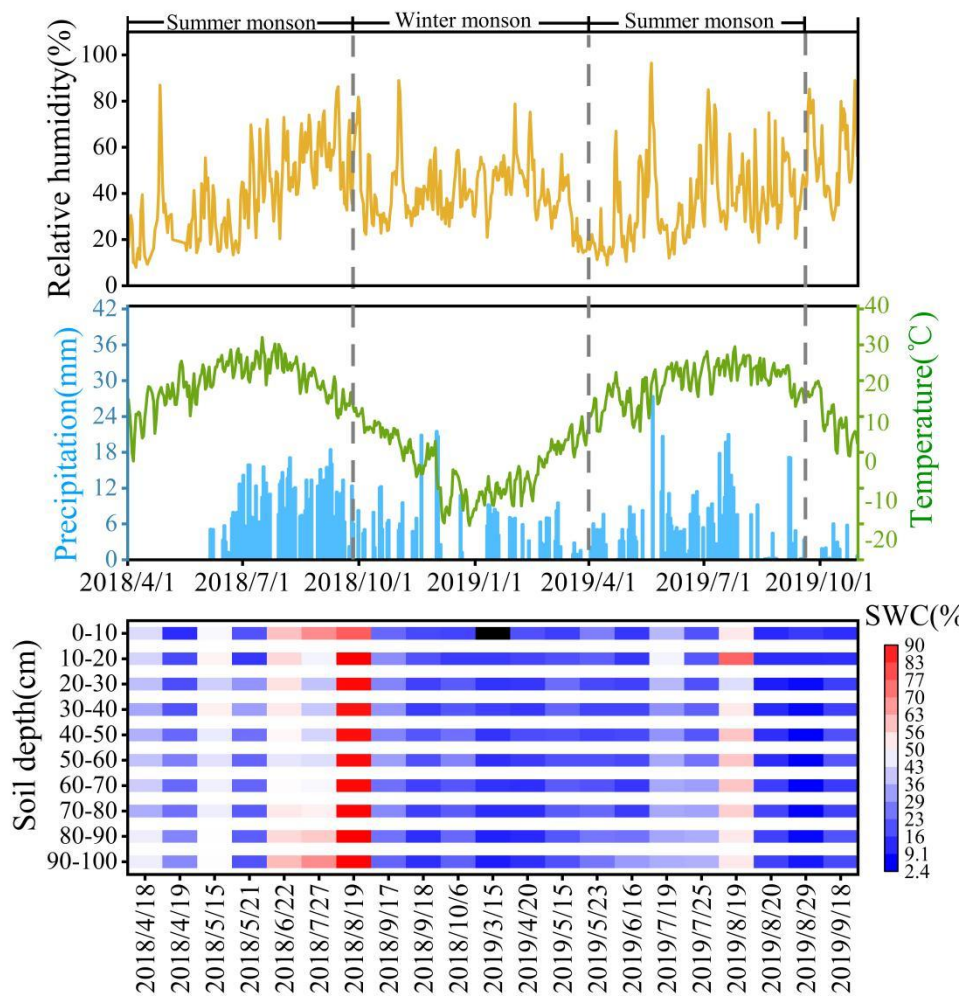


Fig. 2 Diurnal variation of relative humidity, precipitation, temperature, and swc (%) from April 2018 to October 2019

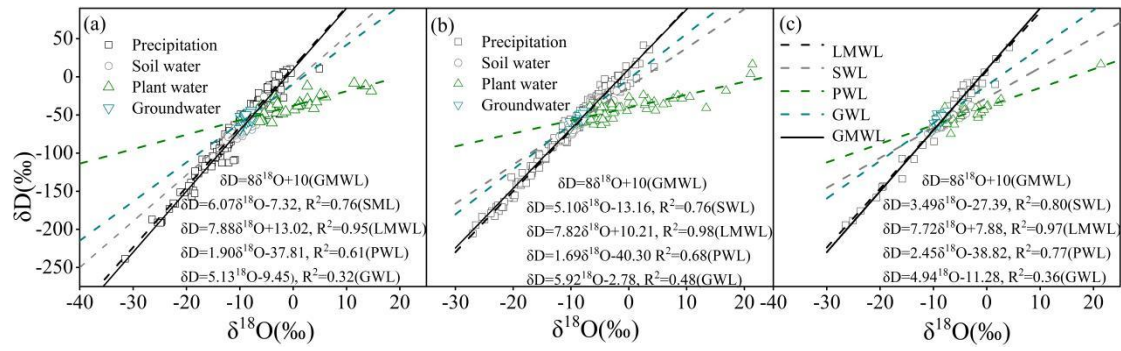


Fig.3 Relationship of stable isotopes in different water bodies in alpine meadow (a), forest (b) and arid foothills (c)

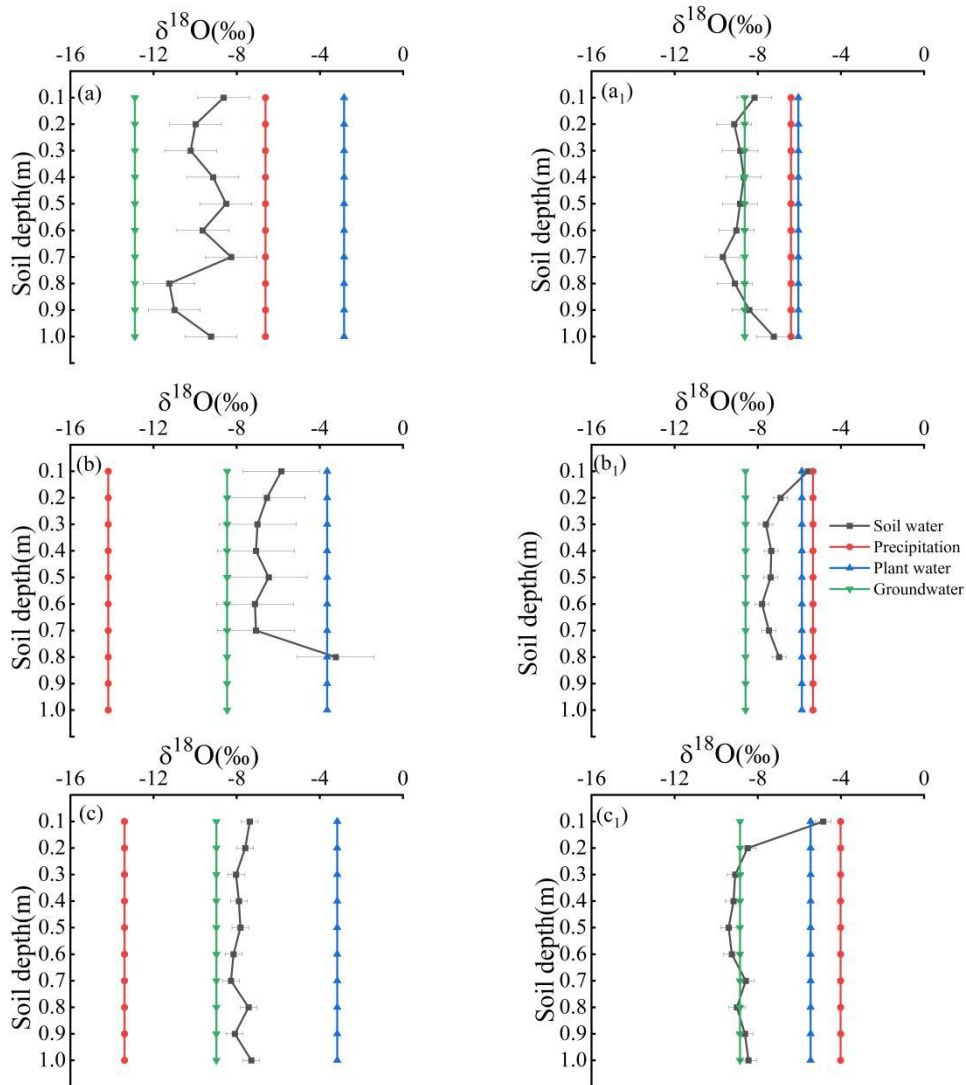


Fig. 4 (a)-(c) represents the variation of  $\delta^{18}O$  of soil, plant, precipitation and groundwater with soil depth in the alpine meadow, forests and arid foothills in the dry season, and (a<sub>1</sub>)-(d<sub>1</sub>) represents the variation of  $\delta^{18}O$  of soil, plant, precipitation and groundwater in the alpine meadow, forests and arid foothills in the rainy season

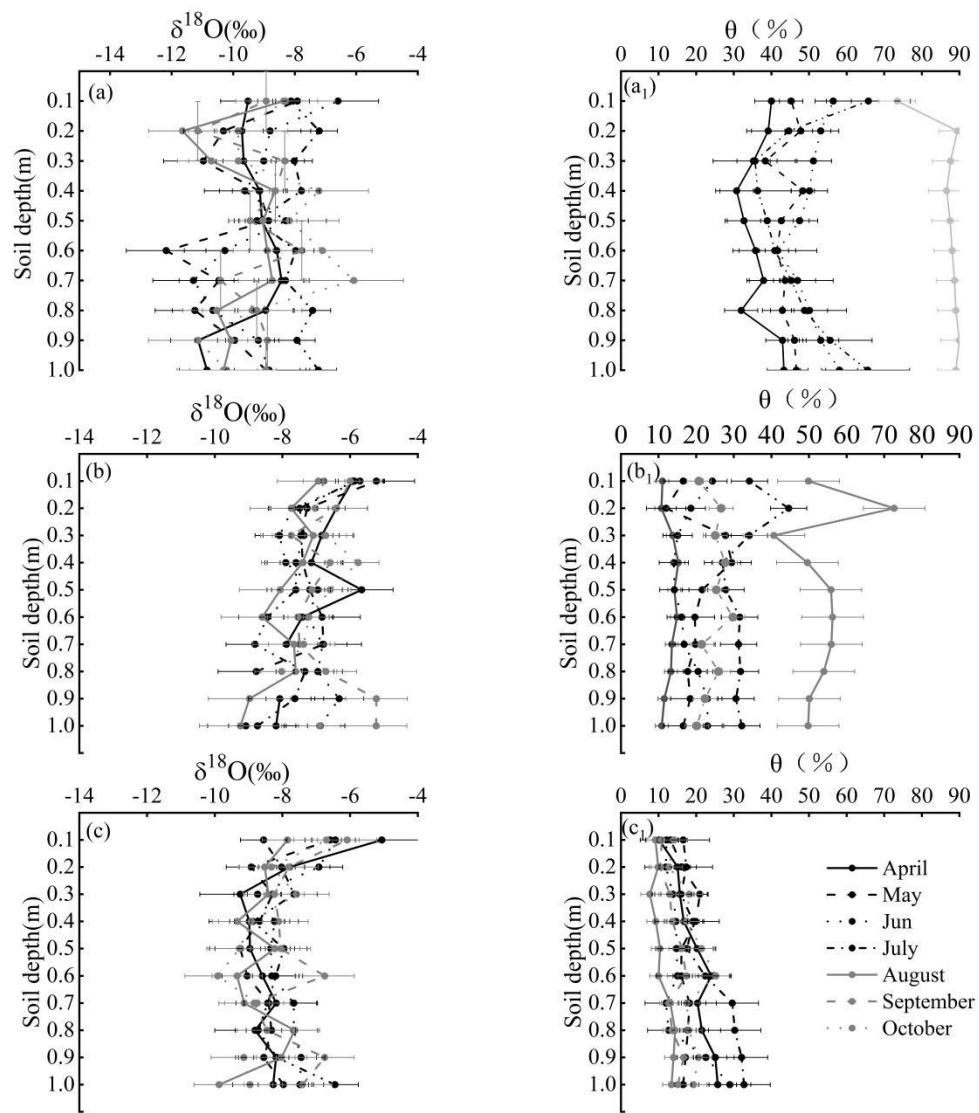


Fig.5 The variation of  $\delta^{18}\text{O}$  and soil water content ( $\theta$ , %) with soil depth. (a)-(c) represent alpine meadow, forests and arid foothills, respectively

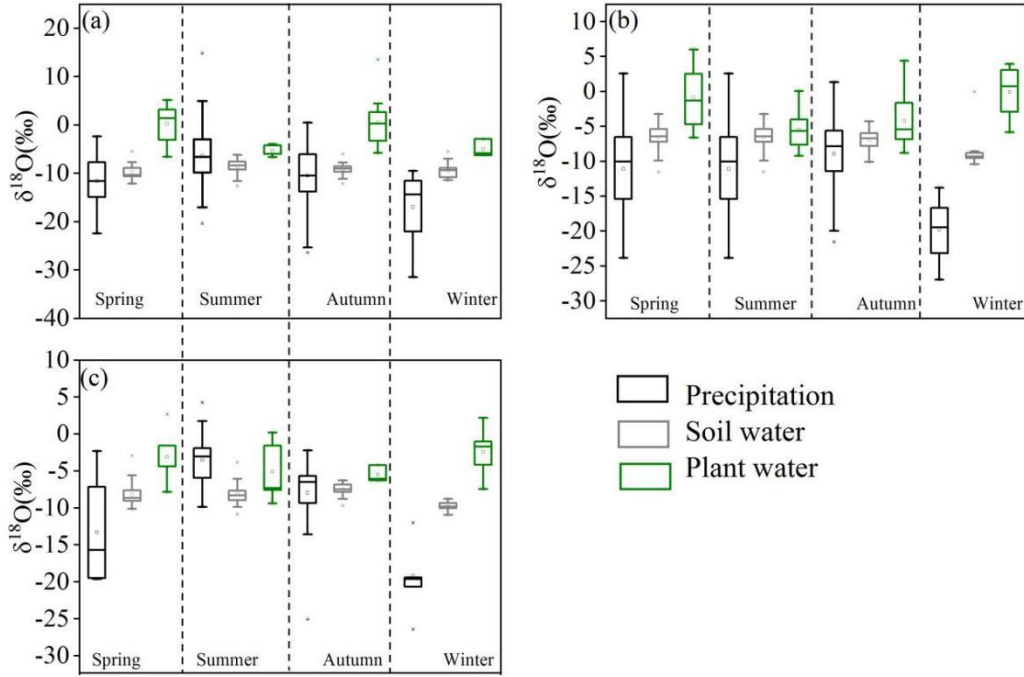


Fig. 6 Seasonal variations of different water isotopes in alpine meadow (a), forests (b) and arid foothills (c)

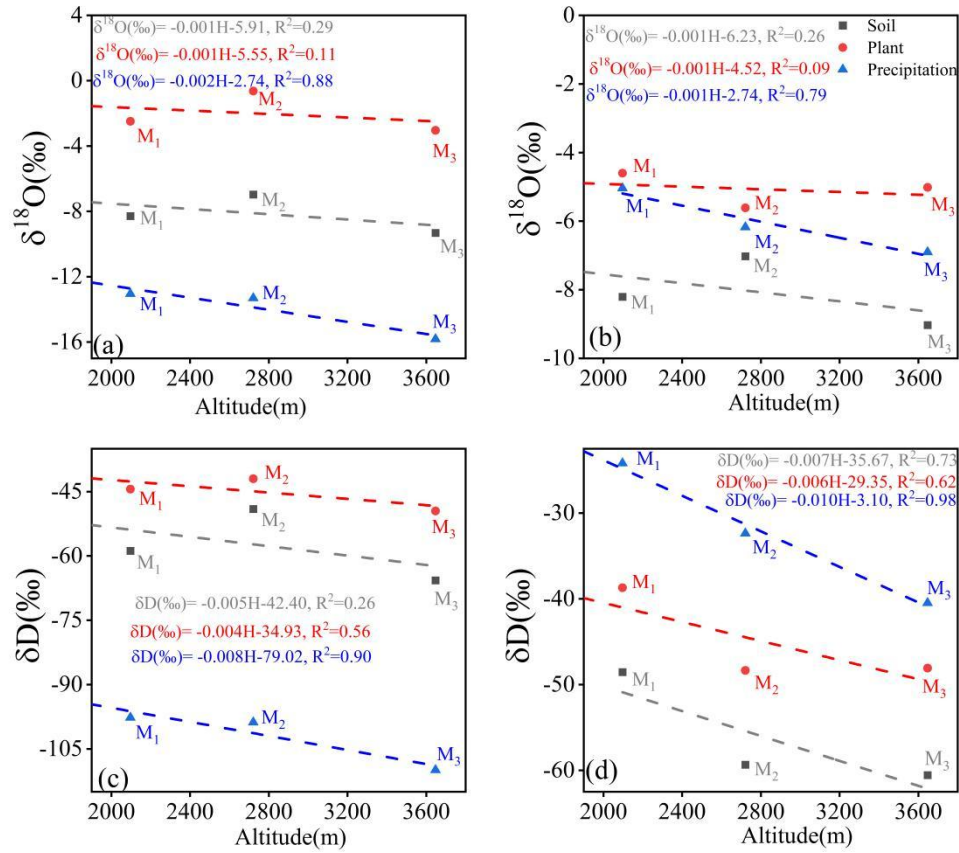


Fig. 7 Relationship between different isotope and altitude in the dry season (a, c) and in the rain season (b, d), M<sub>1</sub> stands for alpine meadows, M<sub>2</sub> stands for forests, and M<sub>3</sub> stands for arid foothills

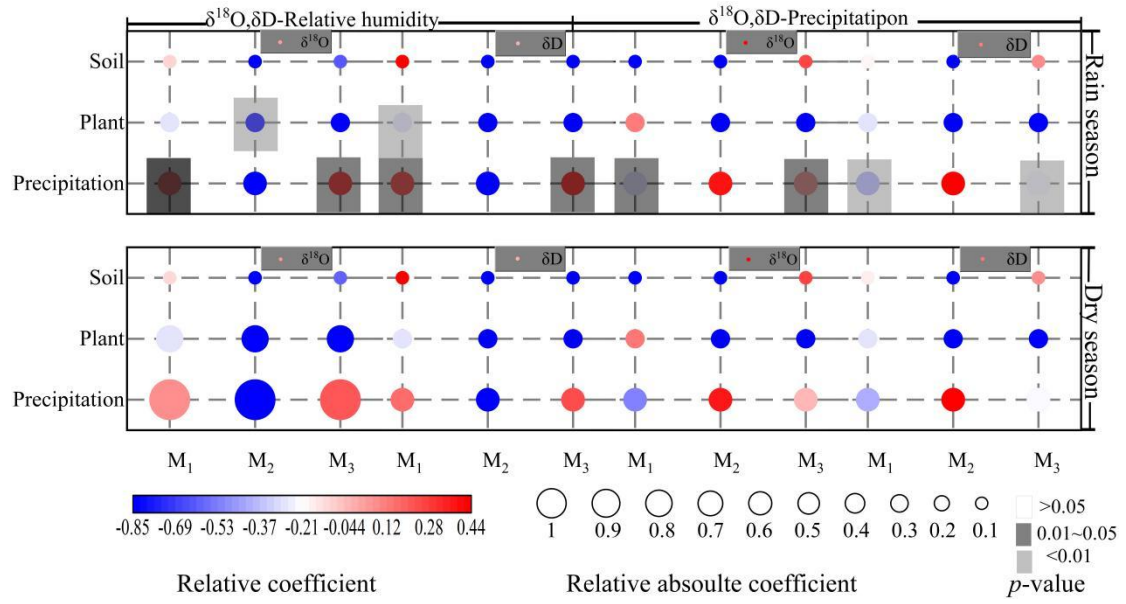


Fig. 8 Relationship between different isotope and relative humidity and precipitation, M<sub>1</sub> stands for alpine meadows, M<sub>2</sub> stands for forests, and M<sub>3</sub> stands for arid foothills

**Table 1 Basic information table of sampling points**

Sampling Station		Geographical Parameters			Meteorological Parameters	
		Longitude (E)	Latitude (N)	Altitude (m)	Average annual temperature (°C)	Average annual precipitation (mm)
M1	Lenglong	101°50'	37°33'	3647	-0.20	595.10
M2	Hulin	101°53'	37°41'	2721	3.24	469.44
M3	Xiying	102°18'	38°29'	2097	7.99	194.67

**Table 2 Comparison of stable isotope of water in different vegetation zones**

Vegetation zone types	Water types	$\delta^{18}\text{O}(\text{‰})$			Coefficient of Variation	$\delta\text{D}(\text{‰})$			Coefficient of Variation
		Min	Max	Average		Min	Max	Average	
Alpine meadow	Precipitation	-31.49	14.79	-9.44	-0.70	-238.62	63.43	-59.43	-0.84
	Soil water	-12.62	-5.46	-9.16	-0.16	-83.86	-26.13	-62.92	-0.16
	Plant water	-6.68	5.12	-1.68	-2.18	-60.22	-12.14	-41.14	-0.28
	Groundwater	-10.07	-7.71	-8.84	-0.07	-68.55	43.72	-54.85	-0.10
Forest	Precipitation	-26.96	4.38	-8.63	-0.74	-205.40	41.35	-60.24	-0.87
	Soil water	-11.96	-0.07	-7.01	-0.25	-78.43	-18.48	-48.68	-0.21
	Plant water	-9.24	5.98	-5.44	-1.31	-63.29	-23.77	-45.12	-0.24
	Groundwater	-10.25	-7.43	-8.56	-0.09	-68.80	-43.75	-53.46	-0.12
Arid foothills	Precipitation	-26.47	4.24	-7.50	-0.87	-194.34	38.62	-48.62	-1.04
	Soil water	-10.98	-2.96	-8.23	-0.15	-74.22	-8.79	-59.17	-0.12
	Plant water	-9.41	2.67	-3.61	-0.88	-74.90	-29.39	-48.79	-0.23
	Groundwater	-10.34	-7.43	-8.88	-0.07	-71.67	-44.26	-55.12	-0.09

**Table 3 Correlation between precipitation isotopes and different temperatures in different vegetation zones**

Vegetation zone type	Correlation below	Correlation between	Correlation above	Correlation during the study period
	0°C	0°C-8°C	8°C	
	$(\delta^{18}\text{O} / \delta\text{D})$	$(\delta^{18}\text{O} / \delta\text{D})$	$(\delta^{18}\text{O} / \delta\text{D})$	
Alpine meadow	0.51*/0.59*	0.30*/0.24*	0.15/0.12	0.59*/0.61*
Forest	0.95*/0.94*	0.66*/0.69*	0.14/0.10	0.69*/0.65*
Arid foothills	0.47/0.51	0.79*/0.71*	0.31/0.14	0.83*/0.81*

**Table 4 Correlation between different isotopes'  $\delta^{18}\text{O}$  and relative humidity and precipitation in different vegetation zones**

Meteorological parameters	Isotope types	Rain season			Dry season		
		Alpine meadow	Forest	Arid foothills	Alpine meadow	Forest	Arid foothills
Relative Humidity	Soil	$y = -0.001x - 8.89$ , $R^2 = 0.001$	$y = -0.03x - 5.21$ , $R^2 = 0.13$	$y = -0.002x - 8.01$ , $R^2 = 0.002$	$y = -0.01x - 8.39$ , $R^2 = 0.03$	$y = 0.01x - 7.21$ , $R^2 = 0.07$	$y = -0.04x - 6.38$ , $R^2 = 0.38$
		$y = -0.11x + 6.11$ , $R^2 = 0.11$	$y = 0.08x - 10.53$ , $R^2 = 0.13$	$y = 0.05x - 7.68$ , $R^2 = 0.04$	$y = -0.09x + 3.78$ , $R^2 = 0.10$	$y = -0.02x - 0.28$ , $R^2 = 0.004$	-
	Precipitation	$y = -0.22x + 9.45$ , $R^2 = 0.28$	$y = 0.02x - 9.50$ , $R^2 = 0.002$	$y = 0.13x + 3.57$ , $R^2 = 0.29$	$y = 0.02x - 16.47$ , $R^2 = 0.002$	$y = 0.16x + 4.33$ , $R^2 = 0.72$	$y = 0.08x - 20.23$ , $R^2 = 0.02$
		Soil	$y = 0.04x - 9.55$ , $R^2 = 0.15$	$y = 0.02x - 7.36$ , $R^2 = 0.01$	-	$y = -0.13x - 8.94$ , $R^2 = 0.18$	-
	Plant		$y = -0.07x - 1.09$ , $R^2 = 0.002$	$y = -0.06x - 5.01$ , $R^2 = 0.01$	$y = 0.18x - 6.00$ , $R^2 = 0.05$	$y = 0.07x - 2.75$ , $R^2 = 0.03$	$y = -0.41x - 0.32$ , $R^2 = 0.06$
		Precipitation	$y = -0.30x - 5.21$ , $R^2 = 0.09$	$y = -0.17x - 6.17$ , $R^2 = 0.05$	$y = -0.28x - 2.84$ , $R^2 = 0.14$	$y = -0.14x - 14.24$ , $R^2 = 0.002$	$y = 0.17x - 9.41$ , $R^2 = 0.11$